JCTC Journal of Chemical Theory and Computation

Assessment of DFT and DFT-D for Potential Energy Surfaces of Rare Gas Trimers—Implementation and Analysis of Functionals and Extrapolation Procedures

Roberto Peverati, Marina Macrina, and Kim K. Baldridge*

University of Zürich, Winterthurerstrasse 190, CH-8057 Zürich, Switzerland

Received February 2, 2010

Abstract: Given the recent developments in methodology associated with the accurate computation of molecular systems with weak interactions, it is of particular interest to revisit systems that are notoriously challenging for determining reliable potential energy surface (PES) descriptions. Additionally, challenges associated with carrying out complete basis set extrapolation procedures and treatment of basis set superposition error (BSSE) are of importance in these descriptions. In this work, investigation into the ability to accurately predict the potential energy surfaces of the main Rg_3 molecules (Rg = He, Ne, Ar) is made across a range of wave function types and large basis sets, including the use of several established extrapolation procedures and counterpoise corrections. Wave function types span most classes of density functional types, including the newest DFT-D schemes, and are benchmarked against high accuracy CCSD(T)/CBS methodology. Study of such systems is valuable, as they serve as simple models for many complex properties, most importantly *n*-body weak interaction energies.

Introduction

Rare gas compounds are, in many cases, simple models for the study of complex properties. In particular, weak interactions of van der Waals bound dimers, *n*-body interaction energies in trimers, tetramers, etc., and complex aggregations of large clusters, are of significant importance. Few-body, rare gas compounds are heavily used for parametrizations of semiempirical potentials, for example, in empirical force fields or *ab initio* molecular dynamics methods. In these cases, highly accurate *ab initio* potential energy surfaces (PES) are extremely important for such parametrizations. Also significant are three-body atomic systems, which present intriguing properties, such as "Efimov physics",[1−4] and "Borromean states",[5,6] with the presence of bound states even when the analogous two-body systems are unbound.

Homodimers present a well-known, simple, one-dimensional PES,[7] commonly used in parametrizations. Equilateral homotrimers present an analogous one-dimensional PES but with a much larger (Borromean) bound state. Because of a less profound knowledge of the nature of the bonding, their use in parametrizations is restricted mainly to three-body correction components.[8,9] For similar reasons, while accurate results of rare gas dimers are used as test systems for theoretical models, homotrimers are very rarely used in this sense.

The study of rare gas trimers is nevertheless a very well established first step in the investigation of the stability of large clusters, and both experimental and theoretical studies have contributed data in this direction.[10−20] Several experimental studies have been carried out on rare gas triatomic systems,[21] indicating less sensitivity in measurements than the weaker binding dimers. There is very little in the literature detailing accurate calculations of the potential energy surfaces of the rare gas trimers, however. Additionally, none of the more recent dispersion-enabled DFT functionals have been tested on these systems, despite their relevance for understanding intermolecular interactions and the implications on the overall computational cost savings compared to traditional benchmark level methods. Rare gas trimers represent ideal candidates for parametrization and validation of new theoretical models, in the same way that dimers have been used up to now.

* Corresponding author tel.: +41 44 635 4201; fax: +41 44 635 6888; e-mail: kimb@oci.uzh.ch.

10.1021/ct100061f
Published on Web 06/25/2010

Table 1. Strategies for Density Functionals beyond GGA

density functional type	main feature	examples	reference
meta-GGA	depend on the Kohn−Sham kinetic energy density	M0X family τ-HCTH family BMK	Zhao et al.[22−25] Handy and Boese[26] Boese/Martin[27]
range-separated hybrid (RSH)	Coulomb operator is separated into long-range and short-range terms, the extent of which determines the exact variant of the functional	LC-BLYP, CAM-B3LYP HSE ωB97	Savin et al.[28,29] Scuseria and Heyd[30,31] Chai and Head-Gordon[32]
empirical/semiempirical	vdW dispersion interactions described empirically with a damped interatomic R^{-6} potential	B97-D	Grimme[33]
double-hybrid	includes terms derived from correlated wave function methods (e.g., MP2 theory)	B2-PLYP, mPW2-PLYP MC3BB, MC3MPW B2K-PLYP, mPW2K-PLYP	Grimme and Schwabe[34,35] Zhao et al.[36] Martin et al.[37]
Andersson−Langreth −Lundqvist functional	long-range exchange correction scheme together with the Andersson−Langreth−Lundqvist vdW functional	vdW-DF	Langreth et al.[38]

There are now a growing number of theoretical models that are appropriate for treating the structure and properties of weakly bound clusters, enabling greater understanding of the importance and representation of short-, intermediate-, and long-range interaction, particularly since the introduction of entire new generations of approximations for the exchange-correlation potential (e.g., see Table 1 and references therein). The local density approximation (LDA) and its analogue, local spin density approximation (LSDA), as the first approximations to the exchange-correlation potential v_{xc} used by Kohn and co-workers with high success, were particularly applicable in solid-state physics. Initial strategies to improve LDA/LSDA enhanced the exchange-correlation functional terms that depend on the gradient of the density, leading to generalized gradient approximation (GGA) functionals. Despite their great success, GGA approximations fail in the description of properties that depend mainly on the correlation of electrons, such as is the case for rare gas trimer complexes. To overcome the main limitations of GGA functionals, various strategies have been developed (Table 1), which offer a high degree of reliability in these cases.

In this work, we have evaluated the latest dispersion sensitive density functional theory (DFT) based methodologies for their ability to accurately represent the potential energy surfaces for a series of rare gas trimer systems. After establishing MP2, CCSD, and CCSD(T) benchmark potentials, a general assessment of DFT trimer potential energy surfaces is made. Two technical issues concerning grid size and BSSE are addressed, before concluding remarks.

Theoretical Methodology and Approach

All calculations reported here used a locally modified version of the GAMESS electronic structure program, running on our group cluster hardware. Associated visualization and analysis was carried out using MacMolPlt[39] and Qutemol.[40] In the present work, we apply our recently implemented semiempirically corrected density functionals,[41] in addition to key functionals implemented by several other GAMESS DFT contributors. Moreover, to carry out a full analysis on the series of rare gas trimers across various classes of density functional types, we have implemented a large variety of additional functionals of different class types. In the process, we have facilitated testing of parameters, future implementations of new functionals, updates of existing functionals, and, from the earlier work, the ability to include the semiempirical dispersion correction in various functionals. Initially, two new routines for the calculation of the B97 family of functionals[42−45] were implemented. The B97-D functional is a special reparameterization of the original Becke 1997 functional,[42] produced by Grimme[33] with the purpose of avoiding the effect of double-counting in the vdW region. The power expansion series coefficients of the original functional description were optimized by Grimme to restrict the density functional representation of the shorter electron correlation ranges, while the medium- to long-range representation is handled by the semiempirical correction term.

Following the formulation of the original B97 functional,[42] we separate exchange and correlation contributions. For the correlation, a FORTRAN routine was generated via a modified version of the *dfauto* program of Knowles et al.[46] The expansion in the gradient up to five terms was used, and the numerical coefficients were passed to the routine as parameters. This correlation routine enables calculation of correlation energy for all implemented functionals. The exchange component of the B97 functional has been implemented as a separate routine, composed of three distinct blocks, (1) the LSDA component, implemented using the previous LSDA routine of GAMESS that includes the range-separation of the Coulomb operator (for the ωB97 family of functionals), (2) the GGA component, implemented using the modified *dfauto* program, as done for the correlation component, and (3) the τ-dependency for the τ-HCTH family of functionals. All three components are accumulated together appropriately, and the global functional derivatives are calculated using a simple chain-rule formula. The new routines enable the implementation of a large number of different reparameterizations of the same basic functional form, and because of their modular nature, new sets of parameters can be easily added in the future, either for the purpose of refinement of the existing formulations based on

new data or for the formulation of new functionals. In addition, our recent implementation of semiempirical dispersion correction capabilities[41] can also be readily accessed for the functionals, enabling, for example, the B97-D and the ωB97X-D dispersion corrected forms.

Several functionals are hybrid functionals, with the percentage of HF exchange appropriately added via an array value option. The range-separated HF and DFT exchange of the RSH functionals are calculated with the long-range correction scheme of GAMESS, but using a slightly modified routine to allow the multiplication with the GGA correction. The LR-HF integrals are calculated directly using Savin et al.'s operator[47] in the two-electron integrals module of GAMESS. According to the formula of Head-Gordon and Chai,[32] the ωB97X functional is calculated as

$$E_{XC}^{LC-GGA} = E_X^{SR-GGA} + E_C^{GGA} + E_X^{LR-HF} + c_x E_X^{SR-HF} \quad (1)$$

The scaled SR-HF exchange for the ωB97X functional is obtained in our implementation indirectly by using the factorization of the total HF exchange (calculated without Savin et al.'s modified Coulomb operators) as

$$c_x E_X^{SR-HF} = c_x(E_X^{HF} - E_X^{LR-HF}) \quad (2)$$

The ωB97X functional is then implemented in a slightly unconventional way, as

$$E_{XC}^{LC-GGA} = E_X^{SR-GGA} + E_C^{GGA} + (1 - c_x)E_X^{LR-HF} + c_x E_X^{HF} \quad (3)$$

This particular reformulation of the functional definition of eq 1 provides additional insight, since it shows more clearly the similarities between the range separated hybrids and the simple meta-GGA functional form of τ-HCTH, as well as other derived functionals.

$$E_{XC}^{meta-GGA} = E_X^{GGA} + E_C^{GGA} + E_X^{\tau} + c_x E_X^{HF} \quad (4)$$

In eq 3, in fact, the τ-dependent term of eq 4 is substituted by the long-range Hartree−Fock term (nonlocal by definition), and the GGA exchange is limited to short-range in eq 3. The other terms, the GGA correlation and the scaled HF exchange, are exactly the same for both functional forms. Written in this form, it is also clear that ωB97 is closely related to nonhybrid functionals ($c_x = 0$), while ωB97X is related to hybrid functionals ($c_x \neq 0$). A summary of all B97-related functionals available in the new release of GAMESS through the described new routines can be found in the Supporting Information.

Evaluated functionals for the present work include **B97**,[42] **B97-1**,[43] **B97-2**,[45] **B97-3**,[44] **B97-D**,[33] **B98**,[48] **HCTH/93**,[43] **HCTH/120** and **HCTH/147**,[49] **HCTH/407**,[50] ***τ*-HCTH**,[26] ***τ*-HCTHhyb**,[26] **BMK**,[27] ***ω*B97** and ***ω*B97X**,[32] ***ω*B97X-D**,[32] BLYP,[51−53] B3LYP,[22,54,55] B2-PLYP,[34] CAM-B3LYP,[29] VS98,[56] PKZB,[57] TPSS,[58,59] TPSSH,[60,61] TPSSM,[62] M05,[22] M05-2X,[63] M06 and M06-2X,[24] M06-L,[64] M06-HF,[65] and M08-HX and M08-SO.[25] The functionals in bold are our most recently implemented functionals to the GAMESS suite. All computations have been carried out using the (96, 1202) Lebedev grid[66] (called the '*army*' grid in GAMESS), and an additional set using the (400, 770) Lebedev grid. A general grid convergence investigation was carried out for the meta-GGA functionals using several other grid specifications as detailed in the text. In accord with our previous study on the performance of the B97-D functional,[41] the scaling factor for the semiempirical dispersion was taken as $s_6 = 1.00$ for all the double-ζ basis sets considered and $s_6 = 1.25$ for all the triple-ζ basis sets considered. Basis set superposition error (BSSE) is corrected with the counterpoise (CP) method.[67] A detailed analysis of the BSSE results is also reported in this work.

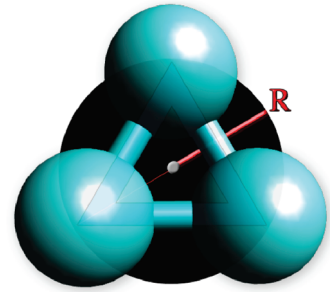

Figure 1. Radial coordinate of the Rg_3 D_{3h} trimer molecule.

In addition to density functional theory, computations were carried out using Hartree−Fock (HF); Møller−Plesset perturbation theory of order 2 (MP2);[68] coupled-cluster with single and double excitations (CCSD);[69] and two methods of coupled-cluster with single, double, and iterative triple excitations CCSD[T] (also known as CCSD+T(CCSD)[69]) and CCSD(T),[70,71] as implemented in GAMESS. The latter is the highest level of theory applied in this study, and arguably one of the best methods available for single-reference computations.

Several basis sets were employed in this study in order to investigate consistency and predictability across the full set of molecules studied. The basis sets include the correlation consistent basis set of Dunning,[72] with augmented functions, denoted aug-cc-pV*n*Z, with n = D for double, T for triple, Q for quadruple, and 5 for quintuple, as implemented in GAMESS (*g* functions for He and *h* functions for Ne and Ar are dropped for aug-cc-pV5Z). We note that relative contractions for each split shell differ from He to Ne and Ar and refer readers to the original articles for more details. Extrapolation to the complete basis set (CBS) limit has been carried out for He_3.

Coupled Cluster Reference Calculations

The potential energy surfaces (PESs) of three Rg_3 systems (Rg = He, Ne, Ar) have been investigated with high-level computational methods up to CCSD(T) with complete basis set extrapolation (CBS). The potential energy surface of each D_{3h} Rg_3 molecule is determined with respect to the ground state of the three separated Rg atoms along the radial coordinate of the trimer (Figure 1). In greater detail, the He_3 molecule is used to carefully investigate performance across all methods, the results of which are then extended to the other two systems, Ne and Ar trimers. For highly accurate comparison, we carry out an extrapolation to the complete

basis set limit with coupled cluster, as described in the next sections, for all three trimers.

Convergence Studies for the He_3 Trimer. Accurate calculations have been carried out for He_3 at the CCSD(T) level of theory, establishing convergence of the PES with respect to increasing basis set size, including extrapolation to the complete basis set limit. Additional calculations were carried out with the aug-cc-pVnZ ($n = 2-5$) series to investigate the convergence properties of this family of basis sets. The correlation consistent basis sets of Dunning and co-workers are used to minimize error associated with finite one-particle expansions. These together with extrapolation to the complete basis set (CBS) limit provide high accuracy for electronic energies, enabling quantitative comparison between different *ab initio* methods.

An important component in establishing reliable potential energy surface data involves consistent extrapolation to complete basis set and complete correlation limits.[72−90] While there has been much discussion associated with carrying out complete basis set extrapolation procedures in the literature across a variety of molecular systems, including challenges associated with the type of molecule, family of basis sets being used, treatment of BSSE, and/or properties being extrapolated, the most accurate and reliable extrapolation methodology is not a matter of consensus. In this work, we compare several of the important extrapolation schemes used in the literature, and therefore we first briefly discuss the different approaches in what follows.

The original purpose of Dunning[72] in the construction of the aug-cc-pVnZ basis sets was to enable the extrapolation of properties using a simple three-points exponential formula, denoted here as [n,n',n'';Feller]-CBS, with [n,n',n'', the cardinality of the employed basis]:

$$f(n) = f^{\mathrm{CBS}} + A\exp(-Bn) \tag{5}$$

where n is the cardinal number of the basis set, for example, $n = 2$ for DZ, 3 for TZ, etc.; $f(n)$ is the property (in this case, energy) obtained using the aug-cc-pVnZ basis set, and f^{CBS} is the extrapolated value for the same property. Several authors assert that eq 5 is suitable for the extrapolation of energies at the Hartree−Fock (HF) level, while in many cases the effective decay for a correlated method (e.g., coupled-cluster) is reasonably slower than the exponential decay.[75,88]

Many other extrapolation techniques have been developed as alternatives to [n,n',n'';Feller]-CBS. In 1962, Schwartz[86] proposed an extrapolation procedure for energies of atoms that incorporates an inverse power series function of the basis set extension, n. While this extrapolation has quite a simple expression for atoms, it tends to become very complicated for molecules containing different types of nuclei, requiring further approximations.[79,91] In the simple case of the helium homotrimer, however, such a formulation can be applied as

$$E(n) = E^{\mathrm{CBS}} + An^{-3} + Bn^{-5} + Cn^{-7} + \ldots \tag{6}$$

Truncation of eq 6 leads to simple n-points formulas. In the present study, we denote the simple two-point formula as [n,n';Schwartz]-CBS, the three-point formula as [n,n',n'';Schwartz]-CBS, and so on.

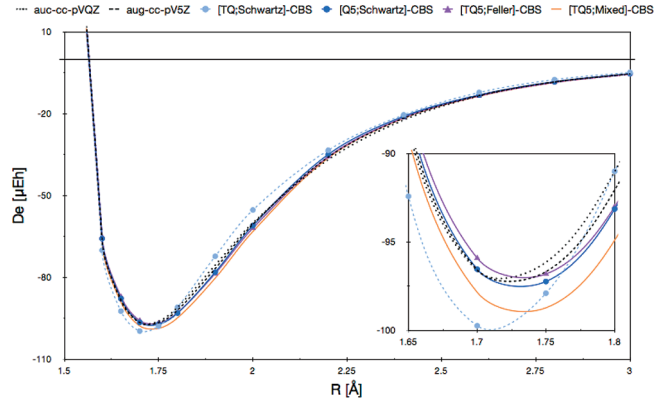

Figure 2. CCSD(T) dissociation energies D_e (μE_h) of the He_3 molecule along the radial coordinate R (Å) as a function of the basis set and CBS extrapolation formula. Dashed black lines are aug-cc-pVQZ and aug-cc-pV5Z.

Table 2. Convergence of Dissociation Energies D_e (μE_h) at the Equilibrium Distances R_{min} (Å), as a Function of Extrapolation Formulas (from above, converging to the middle), and Wave Function Method (from below, converging to the middle)[a]

basis set	wave function	D_e (μE_h)	R_{min} (Å)
aug-cc-pVQZ		−96.165	1.72
aug-cc-pV5Z		−96.696	1.72
[TQ;Schwartz]-CBS	CCSD(T)	−99.753	1.71
[Q5;Schwartz]-CBS		−97.253	1.73
[TQ5;Mixed]-CBS		−98.739	1.74
[TQ5;Feller]-CBS	CCSD(T)	−96.829	1.74
	CCSD[T]	−96.843	1.74
[TQ5;Feller]-CBS	CCSD	−84.872	1.74
	MP2	−66.325	1.80
	HF	−0.261	2.80

[a] The [TQ5;Feller]-CBS/CCSD(T) method is chosen as the reference for all subsequent calculations.

Also of interest here is the extrapolation technique proposed by Truhlar[88] and by Halkier et al.,[75] which couples HF together with correlation methods to obtain a formulation of the type

$$E^{\mathrm{CBS}}(\mathrm{TOT}) = E^{\mathrm{CBS}}(\mathrm{HF}) + E^{\mathrm{CBS}}(\mathrm{corr}) \tag{7}$$

The HF component, E^{CBS}(HF), and the correlation component, E^{CBS}(corr), are obtained using different power expansion extrapolations for their respective methods. In the method of Truhlar, a power expansion n^{-A} with variant coefficients is used, while Halkier et al. use an exponential +Schwartz-type expansion. In the present work, we also employ a hybrid three-point Feller exponential formula for the HF component, [TQ5;Feller]-CBS, together with a three-point Schwartz formula, [TQ5-Schwartz]-CBS, for the correlation component. This method will be denoted simply as [TQ5;Mixed]-CBS.

Results for all extrapolation techniques at the CCSD(T) level of theory are presented in the Supporting Information and only summarized here in Figure 2 and Table 2 for the He_3 trimer system. Comparing results without extrapolation using aug-cc-pVQZ and aug-cc-pV5Z basis sets, one observes evidence of reaching the complete basis set limit. A suitable extrapolation technique with these large basis sets

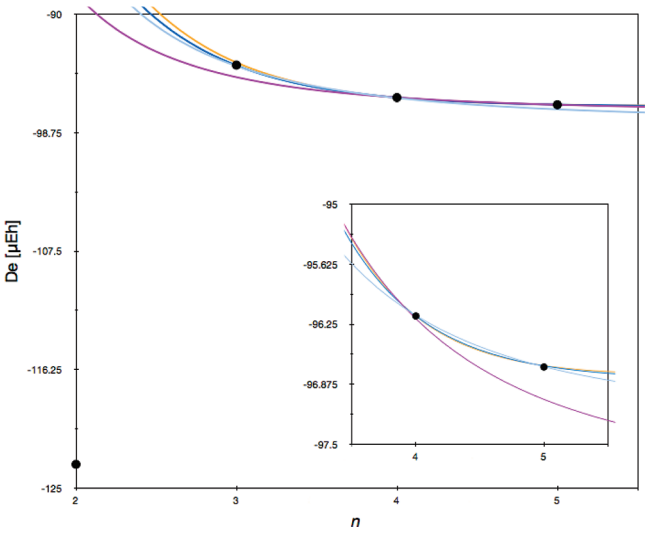

Figure 3. Evaluation of extrapolation formulas at the complete basis set limit as a function of the basis set size, *n*, for He_3 at $R = 1.75$ Å.

should therefore provide results very close to that of the complete basis set limit. The simple two-point [TQ;Schwartz]-CBS extrapolation method, although an improvement over formulas containing double-ζ basis sets (e.g., see the Supporting Information), which are completely outside a monotonically decreasing behavior, still shows substantial error in the minimum region (Figure 2, inset graph). The best results are achieved with the exponential [TQ5;Feller]-CBS and the simple two-point [Q5;Schwartz]-CBS extrapolation procedures.

Basis set convergence and overall extrapolation behavior can also be viewed by evaluating the interaction energies at a fixed distance near the minimum, $R = 1.75$ Å (Figure 3). Figure 3 shows that the convergence of the He_3 trimer energy with the aug-cc-pV*n*Z basis sets is very well approximated by the original exponential formula of Feller. These results are perhaps not a great surprise due to the simple nature of the high-symmetry trimer, with only six electrons. For similar reasons, however, the mixed extrapolation technique appears to be slightly overbound for this simple case, while it might provide more accurate results for more complicated molecular systems. The Feller extrapolation formulation will be used for the other trimer systems in the series.

We next consider optimization of the wave function method, including Hartree−Fock (HF) up to coupled cluster methods. In particular, the dissociation energies, D_e, of the He_3 trimer along the radial coordinate R are calculated using the [TQ5;Feller]-CBS extrapolation with different wave function methods. The full set of computational results across all different wave function types considered can be found in the Supporting Information and is only summarized here in Figure 4 and Table 2.

From the results, we find that HF predicts an essentially unbound system, as expected. MP2 theory shows differences on the order of 30 μE_h in the region of the minimum, with respect to the more accurate wave function types. As such, both HF and MP2 wave functions are largely insufficient for the description of the PES of this trimer. A slight improvement is observed with CCSD, which shows a

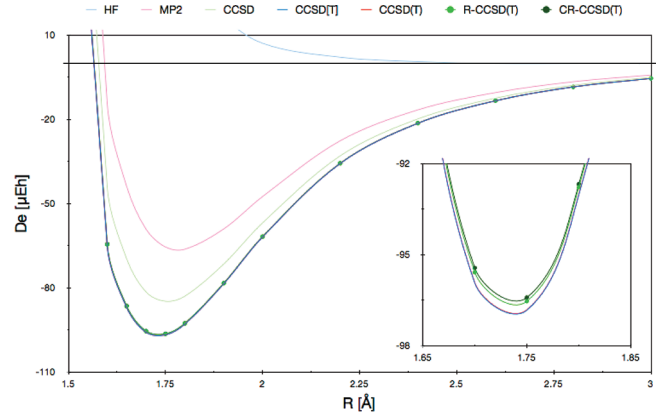

Figure 4. Dissociation energies D_e (μE_h) of the He_3 molecule along the radial coordinate R (Å) using the [TQ5;Feller]-CBS extrapolation procedure as a function of wave function type.

Table 3. CCSD(T) Reference Dissociation Energies D_e (μE_h) of the Rg_3 Molecules along the Radial Coordinate R (Å) Using the [TQ5;Feller]-CBS Extrapolation Procedure

He		Ne		Ar	
R [Å]	D_e [μE_h]	*R* [Å]	D_e [μE_h]	*R* [Å]	D_e [μE_h]
1.00	16 907.2	1.00	132 743.7	1.00	1 035 602
1.20	3250.1	1.20	25 043.9	1.20	351 542.3
1.40	400.2	1.40	3794.8	1.40	105 027.2
1.60	−65.200	1.60	57.43	1.60	26 759.2
1.65	−87.120	1.70	−310.907	1.80	4589.3
1.70	−95.933	1.80	**−380.858**	2.00	−657.443
1.75	**−96.829**	1.90	−336.865	2.20	**−1354.108**
1.80	−93.023	2.00	−265.582	2.30	−1247.063
1.90	−78.645	2.20	−155.338	2.40	−1068.008
2.00	−61.991	2.40	−97.182	2.50	−881.626
2.20	−35.794	2.60	−62.580	2.60	−714.031
2.40	−21.478	2.80	−41.109	2.80	−458.702
2.60	−13.472	3.00	−27.786	3.00	−296.944
2.80	−8.537	4.00	−4.331	4.00	−50.669
3.00	−5.508	6.00	−0.342	6.00	−3.599

difference on the order of 12 μE_h in the region of the minimum. It is clear that triple excitations are necessary to achieve an accurate description of the trimer system. Both CCSD[T] and CCSD(T) show essentially the same description in the region of the minimum, on the order of 0.02 μE_h.

CCSD(T)/[TQ5;Feller]-CBS Calculations for He_3, Ne_3, and Ar_3 Trimers. From the conclusions obtained for He_3 in the previous sections, the potential energy surfaces for all three Rg_3's are determined, using the CCSD(T) method and the [TQ5;Feller]-CBS extrapolation, as detailed in Table 3. The predicted minimum radial coordinate distances are 1.75 Å, 1.80 Å, and 2.20 Å, for He_3, Ne_3, and Ar_3, respectively. The dissociation energies show the significant difference in binding characteristics along this series. In particular, while the radial distance difference between the He_3 trimer and Ne_3 trimer is only 0.05 Å, the difference in dissociation energy is 284 μE_h. Progressing to the Ar_3 trimer, the radial distance increases by a significant amount, 0.40 Å (0.45 Å), as does the dissociation energy, with a difference of 973 μE_h (1257.3 μE_h), compared to Ne_3 (He_3). These reference calculations will be used in the comparative analysis across density functional classes discussed below.

We should point out that the largest source of error in the reported data in Table 3 is associated with the omission of core/valence correlation energies, which would result in some increase in these numbers. Comparison with the limited data in the literature is very difficult due to the different focus of the studies, resulting in a wide variation in predicted energetics across this set of trimers. This has less to do with the quality of results presented in the literature than the fact that the reference state used is quite different from one investigation to another (e.g., referenced with respect to the energy of the three separated atoms, to the energy of the respective dimer plus atom, to the three-body components, etc.). There is also considerable variance in the reporting of internal coordinates for the systems. This lack of consistency limits reliable comparison, and for our current purpose, it is only necessary to have one consistent set of data to benchmark against the variety of DFT functionals.

One might, however, consider comparison with the corresponding rare gas dimers, which instead emphasizes the much larger energies found for the trimers. Full-CI results of van Mourik and van Lenthe report a binding energy for He_2 of 34.68 μE_h at 2.96 Å,[92] data in accord with those proposed by Komasa and Rychlewsky using an explicitly correlated Gaussian function approach.[93] Other calculated values range from those obtained by Hobza and co-workers (32.2 μE_h with CCSD(T) level, 30.32 μE_h with Full-CI level[94]), to 35.02 μEh obtained by Szalewicz and co-workers using SAPT calculations.[95] A more detailed discussion by Specchio et al.[96] on the full set of available potentials can also be found. An accurate analysis of the potential energy surface of Ne_2 was conducted by Gdanitz.[97] The reported binding energy is 131.53 μE_h at $R = 3.10$ Å. Other accurate calculations on this system range from the 130.33 μE_h at $R = 3.10$ Å of Cybulski and Toczłowski (aug-cc-pV5Z+bonding function/CCSD(T) level)[98] to 133.96 μE_h at $R = 3.09$ Å.[99] Finally, Aziz reported the most accurate value to date for Ar_2, 453.99 μE_h at $R = 3.75$ Å, obtained using a semiempirical potential fit to accurate measured data, within experimental error.[100] With a comparison across this set of reported dimers, one can see a relatively consistent 33−34% increase in interaction energy for the trimers from that of the respective dimer system, which is quite substantial.

DFT Potential Energy Surfaces of Rare Gas Trimers

Performance across several density functional class types for the prediction of the potential energy surfaces of the Rg_3 trimers, as referenced against the accurate CCSD(T) [TQ5;Feller]-CBS extrapolated results, is provided in Table 3. The aug-cc-pVnZ family of basis sets, with n = D and T, is used for all reported calculations here, in combination with 34 different exchange-correlation functional approximations. The ultrafine (96, 1202) (corresponds to the "*army*" grid in GAMESS) and (400, 770) Lebedev grids[66] have been used for all calculations. Basis set superposition error (BSSE) is accounted for using the counterpoise (CP) method[101] and further elaborated upon in the discussion.

To facilitate evaluation of the performance of each functional, a mean absolute deviation with respect to the accurate CCSD(T)/CBS data (Table 3) has been calculated on the usual 15-point grid used for the PES calculation. For this evaluation, one could argue that the mean absolute deviation, MAD, evaluated as

$$\mathrm{MAD} = \sum_{X=1}^{X_{\mathrm{tot}}} \left| \frac{D_e^{\mathrm{xc}}(X) - D_e^{\mathrm{CCSD(T)}}(X)}{X\mathrm{tot}} \right| \qquad (8)$$

is not the best parameter for evaluation of the functional performance, due to the fact that it accounts for equal weighting of each point on the grid. To establish a single reliable evaluation parameter for the problem at hand, errors in the region of the minimum should count more than errors in regions far from the minimum. For example, points in the repulsive region at short-range should be more heavily weighted. For this reason, a weighted mean absolute deviation, denoted wMAD, is calculated in addition to the usual MAD. The wMAD values are calculated by giving a weight factor to each point of the grid according to the distance of that point from the equilibrium, and the relative shape of the accurate PES. The weight factors are calculated with the CCSD(T)/CBS PES by scaling each point according to the relative heights of the PES at that point and by renormalization of the total weight to the total number of points in the grid (see the Supporting Information).

In addition to the mean absolute deviation parameters, the difference from the absolute CCSD(T)/CBS value (deviation from reference, abbreviated DFR) in the region of the minimum ($R = 1.75$ Å for He_3, $R = 1.80$ Å for Ne_3, and $R = 2.20$ Å for Ar_3) is also determined in the evaluation of the performance of each density functional approximation. The MAD and wMAD values with respect to the accurate PES for 34 different DFT functionals and two basis sets are collected in Table 4 for He, Ne, and Ar.

For the He_3 trimer, the two functionals that appear to perform the best are the τ-HCTHhyb and ωB97X functionals. Relative to the majority of the data, reasonable performance is also obtained with several of the other functionals, including B97, B97-2, B98, TPSS, TPSSH, M05 and M05-2X, M08-HX and M08-SO, and ωB97X and ωB97X-D. Interestingly, the semiempirical dispersion correction does not seem to improve the results in the two cases it was used, B97-D and ωB97X-D, compared to their uncorrected counterparts. In several cases, we also note that the BSSE does not necessarily improve the results, a point that will be revisited below.

Moving on to the heavier trimers, Ne_3 and Ar_3, which have larger atomic polarizabilities than He_2, we see a difference in the trends of the set of functionals. This might be anticipated on the basis of the difference in bonding in these heavier trimers. In the case of the Ne_3 trimer, the B97 family of functionals performs very well, particularly the B98, B97, B97-1, and B97-K functionals. Other functionals also have relatively good performance, including M05, M05-2X, M06-HX and M06-SO, TPSS and TPSSH, and τ-HCTHhyb. However, while the DFR value is fairly low, the wMAD values are noticeably large. Additionally, several of these functionals need to be used with caution given the known spurious oscillatory behavior having to do with the kinetic

Table 4. MAD, wMAD, and Deviation from Reference near the Equilibrium Distance for 34 Different Density Functionals and (a) He_3, (b) Ne_3, (c) Ar_3[a]

	aug-cc-pVTZ		
helium trimer	MAD	wMAD	DFR $R = 1.75$
B97	201.0 (201.8)	65.7 (68.9)	−78.2 (−81.7)
B97-1	132.3 (134.3)	113.6 (116.7)	−125.7 (−128.9)
B97-2	453.5 (449.6)	**43.3 (39.8)**	**32.4 (28.7)**
B97-3	707.1 (690.5)	518.2 (510.9)	583.7 (576.9)
B97-D	679.6 (681.3)	73.3 (78.6)	−102.4 (−108.9)
B97-K	276.9 (283.6)	118.5 (122.3)	−119.8 (−123.2)
B98	134.5 (135.1)	73.4 (76.5)	−84.2 (−87.5)
HCTH/93	1227.9 (1,220.7)	306.2 (298.8)	318.5 (310.4)
HCTH/120	436.9 (438.1)	318.2 (324.2)	−368.1 (−374.7)
HCTH/147	515.3 (515.5)	149.5 (155.7)	−183.6 (−190.5)
HCTH/407	696.9 (700.3)	637.8 (644.9)	−732.7 (−740.4)
τ-HCTH	487.5 (489.9)	271.0 (277.3)	−325.6-(332.7)
τ-HCTHhyb	313.4 (312.0)	**13.9 (15.2)**	**−17.2 (−21.0)**
BMK	1128.9 (1,085.6)	871.6 (854.3)	947.9 (932.3)
ωB97	147.8 (148.2)	185.9 (180.6)	214.1 (208.6)
ωB97X	**31.4 (26.9)**	**13.7 (14.6)**	**−5.6 (−10.6)**
ωB97X-D	549.1 (541.0)	73.3 (71.1)	46.9 (41.8)
BLYP	516.6 (511.1)	400.7 (395.4)	457.1 (451.4)
B3LYP	253.8 (248.9)	258.1 (254.2)	297.7 (293.8)
B2-PLYP	111.4 (112.6)	147.8 (141.6)	174.3 (168.3)
CAMB3LYP	221.7 (221.0)	75.8 (71.2)	95.6 (90.7)
VS98	501.9 (505.4)	224.7 (227.5)	−224.5 (−231.4)
PKZB	796.2 (796.8)	209.3 (216.0)	−256.8 (−264.2)
TPSS	166.7 (166.3)	69.7 (74.4)	−87.1 (−92.6)
TPSSH	141.8 (141.2)	46.0 (49.5)	−58.7 (−63.0)
TPSSM	219.9 (219.3)	87.2 (92.3)	−106.71 (−112.6)
M05	140.3 (148.7)	82.2 (84.5)	−63.1 (−68.8)
M05-2X	128.5 (126.2)	**49.6 (49.1)**	**5.9 (−1.7)**
M06	278.9 (250.0)	317.6 (332.6)	−422.9 (−438.9)
M06-2X	226.7 (226.5)	314.8 (319.2)	−383.5 (−387.5)
M06-L	140.7 (109.8)	60.5 (92.9)	−98.7 (−134.5)
M06-HF	497.4 (492.7)	365.7 (382.3)	−422.9 (−439.3)
M08-HX	104.8 (108.7)	65.3 (61.9)	70.1 (62.5)
M08-SO	**87.9 (54.8)**	**37.8 (42.5)**	**−33.4 (−48.7)**

	aug-cc-pVTZ		
neon trimer	MAD	wMAD	DFR $R = 1.80$
B97	1378.3 (1252.5)	**107.2 (51.5)**	**27.5 (−3.0)**
B97-1	808.5 (735.8)	**50.7 (101.4)**	**−12.6 (−41.7)**
B97-2	1938.4 (1786.4)	391.3 (323.3)	146.7 (106.9)
B97-3	1786.3 (1652.3)	1082.0 (1024.8)	703.9 (668.8)
B97-D	2850.1 (2726.7)	242.8 (266.5)	−390.4 (−430.1)
B97-K	731.6 (689.0)	**147.7 (189.2)**	**12.0 (−13.4)**
B98	980.5 (848.8)	**74.3 (21.6)**	**30.6 (−3.1)**
HCTH/93	4,098.9 (3969.8)	990.5 (931.3)	413.6 (381.5)
HCTH/120	1827.5 (1771.6)	316.0 (365.9)	−314.4 (−341.0)
HCTH/147	2328.1 (2231.7)	133.5 (121)	−114.0 (−142.4)
HCTH/407	2417.0 (2374.8)	840.4 (893.3)	−707.6 (−733.5)
τ-HCTH	2157.1 (1987.3)	187.3 (220.8)	−250.1 (−315.0)
τ-HCTHhyb	1404.2 (1233.8)	259.6 (184.0)	90.9 (45.7)
BMK	1439.0 (1242.8)	1831.5 (1750.6)	1033.8 (974.0)
ωB97	503.4 (464.5)	404.6 (358.5)	402.4 (379.2)
ωB97X	418.2 (275.7)	209.4 (147.0)	187.5 (150.8)
ωB97X-D	1580.1 (1372.4)	326.2 (258.9)	−49.3 (−114.8)
BLYP	1855.3 (700.0)	749.6 (700.0)	579.4 (555.7)
B3LYP	926.8 (445.5)	501.6 (445.5)	415.6 (385.9)
B2-PLYP	454.1 (191.7)	287.4 (191.7)	265.2 (200.4)
CAMB3LYP	499.3 (122.2)	137.9 (122.2)	238.7 (211.7)
VS98	1220.3 (444.0)	457.3 (444.0)	573.0 (548.8)
PKZB	3163.1 (137.6)	125.7 (137.6)	−171.4 (−193.5)
TPSS	1383.9 (112.0)	**157.3 (112.0)**	**−11.1 (−52.3)**
TPSSH	1182.3 (110.6)	**184.0 (110.6)**	**39.0 (−4.5)**
TPSSM	1677.4 (108.4)	138.2 (108.4)	−36.2 (−73.5)
M05	608.8 (193.0)	143.0 (193.0)	79.8 (35.2)
M05-2X	402.3 (219.6)	172.1 (219.6)	134.7 (78.9)
M06	996.4 (269.6)	218.3 (269.6)	−310.1 (−400.5)
M06-2X	552.9 (392.5)	315.5 (392.5)	−306.8 (−356.5)
M06-L	183.7 (303.2)	178.4 (303.2)	−128.4 (−256.4)
M06-HF	551.9 (560.3)	292.9 (560.3)	−410.5 (−655.9)
M08-HX	529.8 (72.5)	214.3 (72.5)	87.4 (−21.3)
M08-SO	590.8 (47.1)	**108.4 (47.1)**	**15.6 (−52.4)**

	aug-cc-pVTZ		
argon trimer	MAD	wMAD	DFR $R = 2.20$
B97	2912.7 (2837.5)	916.3 (848.6)	1268.1 (1186.7)
B97-1	2028.4 (1952.3)	513.2 (445.3)	643.2 (561.0)
B97-2	4035.9 (3955.6)	1466.5 (1395.3)	2101.4 (2015.9)
B97-3	3701.8 (3486.0)	1981.4 (1889.8)	2573.0 (2458.1)
B97-D	4722.7 (4670.1)	377.2 (350.0)	528.0 (439.7)
B97-K	5986.0 (5850.1)	460.5 (403.2)	541.4 (470.4)
B98	2286.4 (2200.8)	773.4 (698.6)	1041.9 (951.7)
HCTH/93	7934.2 (7868.7)	2690.4 (2626.7)	3905.5 (3830.6)
HCTH/120	4941.3 (4938.9)	363.0 (334.0)	539.2 (485.2)
HCTH/147	5610.7 (5,559.5)	1008.0 (956.0)	1479.6 (1418.9)
HCTH/407	5901.9 (5900.4)	733.8 (767.0)	−614.0 (−665.6)
τ-HCTH	6003.0 (5985.4)	773.9 (675.1)	1204.6 (1089.7)
τ-HCTHhyb	3191.2 (3169.4)	1146.1 (1056.9)	1617.8 (1511.5)
BMK	5738.6 (5302.1)	3258.8 (3090.5)	4430.9 (4217.3)
ωB97	1015.7 (1021.3)	658.0 (616.8)	581.1 (489.8)
ωB97X	**729.9 (733.2)**	**242.6 (205.4)**	**80.9 (−9.9)**
ωB97X-D	2114.3 (1991.7)	666.3 (569.4)	1087.3 (957.5)
BLYP	4259.9 (4,185.0)	2293.3 (2226.4)	3077 (2998.8)
B3LYP	3402.2 (3248.0)	1780.2 (1713.6)	2369.9 (2290.3)
B2-PLYP	2517.8 (1979.8)	1086.3 (970.6)	1426.7 (1278.9)
CAMB3LYP	1477.1 (1331.0)	1110.6 (1049.7)	1418.5 (1345.6)
VS98	2732.7 (2706.4)	1778.7 (1813.2)	−2847.6 (−2905.2)
PKZB	5547.3 (5502.8)	1089.1 (1041.2)	1615.0 (1559.5)
TPSS	3294.5 (3268.6)	1204.5 (1119.3)	1766.3 (1665.3)
TPSSH	2822.0 (2794.2)	1208.2 (1123.2)	1751.3 (1650.8)
TPSSM	3455.6 (3371.8)	1194.2 (1116.3)	1753.4 (1661.5)
M05	3157.4 (3072.1)	443.6 (364.9)	425.7 (334.0)
M05-2X	1054.6 (753.1)	**196.6 (120.3)**	**87.3 (−62.6)**
M06	1724.4 (1497.2)	610.6 (439.3)	897.1 (646.2)
M06-2X	621.8 (503.3)	241.0 (167.3)	472.5 (346.0)
M06-L	1456.6 (1157.1)	347.0 (113.5)	436.9 (42.5)
M06-HF	1299.9 (1678.5)	534.8 (351.2)	878.4 (511.3)
M08-HX	1645.6 (1337.4)	719.6 (570.5)	797.6 (598.2)
M08-SO	1639.2 (1279.9)	463.6 (284.3)	496.0 (272.0)

[a] Results shown are BSSE corrected (BSSE uncorrected).

energy density component.[102−104] This is addressed in more detail in the next section.

Finally, for the Ar_3 trimer, we notice that considerably fewer functionals provide reasonable performance. In this case, the ωB97X functional stands out, with the M05-2X functional being also reasonable relative to the other functionals. This would indicate a type of bonding in this trimer that is not well represented by most of these functionals.

Across all trimers, several meta-GGA functionals, such as VS98 and PKZB, show results that are highly dependent on the system as well as the basis set, with acceptable results in many cases, but quite poor results in others. As with the other meta-GGA functionals, these two functionals also show oscillating behavior. The BLYP, B3LYP, CAM-B3LYP, and BMK functionals also have overall poor performance, something that could be a result of specialized parametrization for specific properties, e.g., for kinetic data, rather than

Table 5. M06-L/aug-cc-pVTZ Energy, RMS Gradient, and Computational Time for Ar_3 Trimer, as a Function of Grid Specification

	grid specification		$R = 1.00$ Å			$R = 2.2$ Å		
grid	radial	angular	energy	RMS	CPU	*E*	RMS	CPU
Lebedev SG1	24	1−94 (variable)	−1581.58670477	0.5132730	17.9	D.N.C.[a]		
polar coordinate	96	Theta = 12, Phi = 24	−1581.58369967	0.5142771	11.1	−1582.61268820	0.0004244	5.1
Lebedev default	96	302	−1581.58406747	0.5136053	12.1	D.N.C.		
Lebedev R1,tight	96	590	−1581.58406691	0.5138834	16.7	−1582.61268238	0.0002371	24.6
Lebedev R1,U-tight	96	770	−1581.58409109	0.5139260	17.7	−1582.61270112	0.0002315	31.5
Lebedev R2,U-tight	200	770	−1581.58409833	0.5139036	42.7	−1582.61259280	0.0001795	61.5
Lebedev R3,U-tight	**250**	**770**	**−1581.58409854**	**0.5139029**	**32.6**	**−1582.61259277**	**0.0001564**	**41.3**
Lebedev R4,U-tight	300	770	−1581.58409812	0.5139005	46.3	−1582.61259271	0.0001701	71.7
Lebedev R5,U-tight	400	770	−1581.58409862	0.5138996	63.3	−1582.61259271	0.0001701	71.7
Lebedev Army	96	1202	−1581.58409655	0.5139938	31.9	−1582.61269837	0.0002469	39.6
Lebedev R6, Army	**250**	**1202**	**−1581.58410481**	**0.5139705**	**46.4**	**−1582.61259482**	**0.0001570**	**64.1**

[a] SCF procedure did not converge.

structural, in the case of BMK. The B2-PLYP functional also provides relatively unsatisfactory results in all cases.

Quality of Density Functional Theory Integration Grid. The noted oscillatory behavior observed in several regions of the PES for some of the represented density functionals, in particular the meta-GGA functionals, is not an unknown phenomenon within the context of density functional theory and has been discussed in the literature.[102,103,105−107] Such behavior was discussed in a recent article by Johnson and co-workers,[102] specifically in reference to the meta-GGA functional analysis of the PES for a set of dispersion-bound complexes, including the Ar trimer. This erroneous behavior is thought to originate from the divergence of the τ-dependent term in these functionals. The suggestion from Johnson and co-workers of how to avoid this spurious behavior is to use an ultrafine grid.

To illustrate the effect of grid specification, we have carried out computations using a variety of standard as well as other more and less stringent grid specifications, specifically for the Ar_3 system and the M06-L funtional, which showed oscillatory behavior even when using the relatively stringent army grade grid (96, 1202). Table 5 shows the results for two geometry specifications of the Ar_3, one relatively far from the PES minimum, $R = 1.0$ Å, and a geometry near the PES minimum, $R = 2.2$ Å, where we find a region of some functional oscillation problems. Two types of grid quadratures are represented in the table, an older polar coordinate grid[108] and the newer Lebedev grid.[66] The latter grid has been found to be more efficient for use in DFT, due to the reduction in the number of quadrature points needed to obtain convergence, compared to other grids.[108−110] The exchange, correlation, and kinetic energy correction contributions to the energy are determined by summing the contributions from grids centered on each nuclei.[111,112] The quadrature specification for the angular component is combined with the 1D integration for the radial component and enables the numerical construction of the required integrals. The polar grid specification has been predominantly replaced by the Lebedev grid due to the rather poor distribution of points on the spherical grids, which requires considerably more grid points to obtain a reasonable invariance to rotation.

Analysis of the data in Table 5 shows the sensitivity of the grid to energy, gradient, and associated computational cost, for this functional. In the region specified by $R = 1.00$ Å, a reasonable choice of angular and radial specification (e.g., at least the default (96, 302) specification), shows quite good convergence. Use of a very loose grid clearly results in poor representation of the PES. However, near the observed oscillatory behavior in the PES, $R = 2.2$ Å, one readily sees the need for a tighter grid specification, particularly associated with the angular component. An optimal tight grid choice is typically observed with an angular component of at least 770. Therefore, using 770 or the typical "army grid" specification of 1202 is expected to provide relatively good convergence in structure and property.

The radial grid and associated weights are a function of the Bragg−Slater radius of the atom, and therefore the number of grid points is expected to vary with the atom type. While typical values are 96 (or 99) for most molecules investigated, higher specifications (e.g., 150−250) may be necessary with heavier atoms or, likewise, much smaller grid specifications for very small atoms. However, if overly large radial specifications are made for the particular atom, the points can become so dense and the extent of the spheres so extreme that numerical instabilities can be observed. This is the case, for example, in the raw data of Table 5, where one sees small oscillations in the data beyond a radial specification of about 250. The effect appears to be much smaller than for the angular component (e.g., Figure 5).

Results displayed in Figure 5 show a comparison of data from (400, 770) and (96, 1202) grid specifications for the M06-L functional. Despite the fact that this more extreme nonstandard radial specification provided by a (400, 770) grid provides a much smoother shape of the PES (and in general, for functionals that have oscillations in some areas of the PES), the underlying behavior and overall performance of the affected functionals does not improve. For example, wMAD for He_3 using M06-L is 60.5 with an army grade grid (96, 1202) and 62.3 with a (400, 770) grid; for the TPSS functional, wMAD is 166.7 and 166.1, respectively. This could be indicative of an overly large value for the radial component, which does result in a smoothing of the PES with the use of the tighter grid but likely has too many points, resulting in a small degradation in overall performance.

In a more recent publication by Wheeler and Houk[104] focusing only the M06 suite of functionals, it was concluded that such spurious behavior originates from grid sensitivity in the kinetic energy density enhancement factor used in the

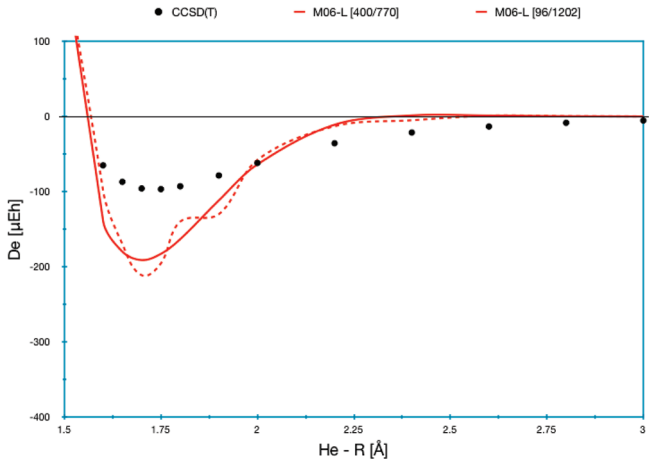

Figure 5. Effect grid size with the M06-L functional for the He_3 potential energy surface.

exchange component of these functionals. While it is clear that the grid specification is quite important, the balance of radial and angular grid specification probably warrants a more systematic investigation, particularly as it is an inherent problem of the meta-GGA class of functionals. In general, sufficiently tight grids should always be used when calculating structure and properties to avoid erroneous behavior.

Assessment of DFT Surfaces. For a global view of the behavior of the series of density functionals, Figure 6 shows the results of PES data for the set of density functional class types. The first class consists of nonhybrid functionals, including B97-D, HCTH/407, and BLYP, as well as τ-HCTH, TPSSH, and M06-L, that are nonhybrid meta-GGAs. The second class consists of a selection of hybrid functionals, as well as range-separated hybrids, including the most complete reparameterization of the B97 functional (called B98), the commonly used B3LYP functional, the double-hybrid B2-PLYP, the range-separated CAM-B3LYP, and the new ωB97 functionals of Chai and Head-Gordon:[32] ωB97, ωB97X, and ωB97X-D. The third class includes a selection of hybrid meta-GGA functionals, including TPSSH, M05, M05-2X, M06, M06-2X, M08-HX, and M08-SO.

For helium, very few functionals provide a dissociation curve close to the reference data. The ωB97X functional is the only functional that comes close to the reference data. Within the local functionals, the meta-GGA M06-L (only with a tight radial specification) and TPSS are the only functionals of the set that present at least a reasonable overall curve shape, albeit strongly overbinding. The B97-D curve is shifted to longer equilibrium geometry and also is strongly overbinding. Many of the common GGA functionals are either dissociative or weakly bound for this system. It is interesting to compare ωB97X, which does a good job close to the minimum, with the dispersion corrected version, ωB97X-D, which shows a drastic shift to longer equilibrium but now has the correct dissociation. The class of hybrid meta-GGA functionals has quite widely variant behavior from one functional to another, making it unclear if any particular result is fortuitous or due to a correct description of the physics. All essentially have defects that would be unacceptable for accurate prediction, which is perhaps disappointing considering the formulation of these functionals. The TPSSH functional has the most reasonable prediction of the whole set, but it is strongly overbinding.

Looking at the classes of functionals for Ne_3, we observe some improvements in functional performance, which may be attributed to the increased binding energy for this heavier rare gas trimer. The M06-L (only with a tight radial grid) and TPSS nonhybrid meta-GGA's again show the most reasonable overall binding curves, albeit now the TPSS functional is slightly displaced to a longer equilibrium position and is underbinding. The B98 hybrid GGA functional is also reasonable, yet slightly underbound. The ωB97X functional in this system now is considerably underbinding, which is corrected with the semiempirical dispersion, but again ωB97X is shifted to a longer equilibrium distance. The performance of meta-GGA functionals is once again far from acceptable, despite some small general improvements.

Finally, we look at the three classes of functionals for Ar_3, which has the largest atomic polarizability of the series. This fact is reflected in the behavior of many functionals, which show more reasonable binding curves in comparison to the other two trimers. In particular, B97-D, M06-L (with a tight radial grid), and τ-HCTH nonhybrid functionals perform well, but HCTH/407 is still overbinding, and TPSS is progressively more under-binding than in Ne_3. Of the hybrid GGA functionals, ωB97X and ωB97-D show again this trend of the former having reasonable prediction around the equilibrium geometry, and the latter only having reasonable dissociation but considerably underbinding. Mostly all of the meta-GGA functionals are underbinding, but many more have overall correct behavior, predicting curves that are at least within the region of the correct reference data, indicating a more correct description of the physics of this system.

Across all systems, the ωB97X functional (with the exception of an estimated underbinding curve for Ne_3) and the M06-L nonhybrid meta-GGA functional with a sufficiently tight radial grid, show a relatively consistent performance across all trimers. It is evident that the choice of the functional as well as the grid extent must be seriously considered for reliable results. It is interesting to note the general very poor behavior of some commonly used functionals, for example, BLYP, B3LYP, and the double hybrid B2-PLYP. For all three rare gas trimers, these three functionals predict a dissociative or very underbinding phenomenon, indicating more general problems than associated with the variation in binding phenomena in the three systems.

Elaboration on BSSE. Looking carefully at the results in Table 4, in some cases, the BSSE uncorrected results are moderately better than those that are BSSE corrected. However, it is well-known that BSSE plays a key role for accurate treatment of weakly bound complexes, where too small basis sets result in poor prediction of binding energies and intermolecular distances.[113,114] Although it is generally believed that DFT is much less affected by BSSE than other wave function types, a basis set of at least triple-ζ quality is typically necessary to significantly reduce the BSSE.[115] The counterpoise correction (CP)[67] is a standard method used to correct for BSSE, and while the procedure itself has an associated error (typically results in an overestimation of

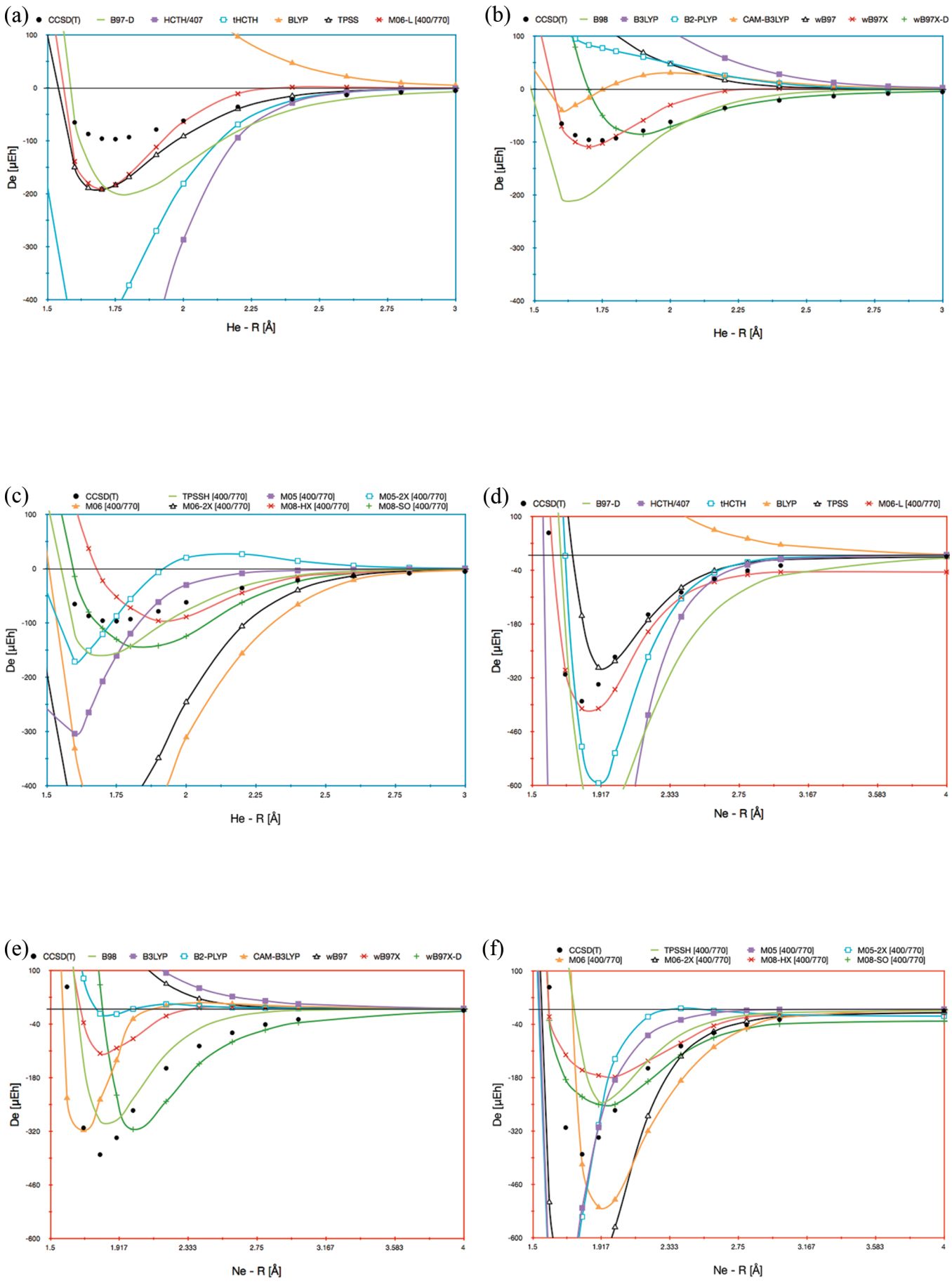
(a)
CCSD(T)
B97-D
HCTH/407
tHCTH
BLYP
TPSS
M06-L [400/770]
De [μEh]
He - R [Å]
(b)
CCSD(T)
B98
B3LYP
B2-PLYP
CAM-B3LYP
wB97
wB97X
wB97X-D
De [μEh]
He - R [Å]
(c)
CCSD(T)
M06 [400/770]
TPSSH [400/770]
M06-2X [400/770]
M05 [400/770]
M08-HX [400/770]
M05-2X [400/770]
M08-SO [400/770]
De [μEh]
He - R [Å]
(d)
CCSD(T)
B97-D
HCTH/407
tHCTH
BLYP
TPSS
M06-L [400/770]
De [μEh]
Ne - R [Å]
(e)
CCSD(T)
B98
B3LYP
B2-PLYP
CAM-B3LYP
wB97
wB97X
wB97X-D
De [μEh]
Ne - R [Å]
(f)
CCSD(T)
M06 [400/770]
TPSSH [400/770]
M06-2X [400/770]
M05 [400/770]
M08-HX [400/770]
M05-2X [400/770]
M08-SO [400/770]
De [μEh]
Ne - R [Å]

Figure 6

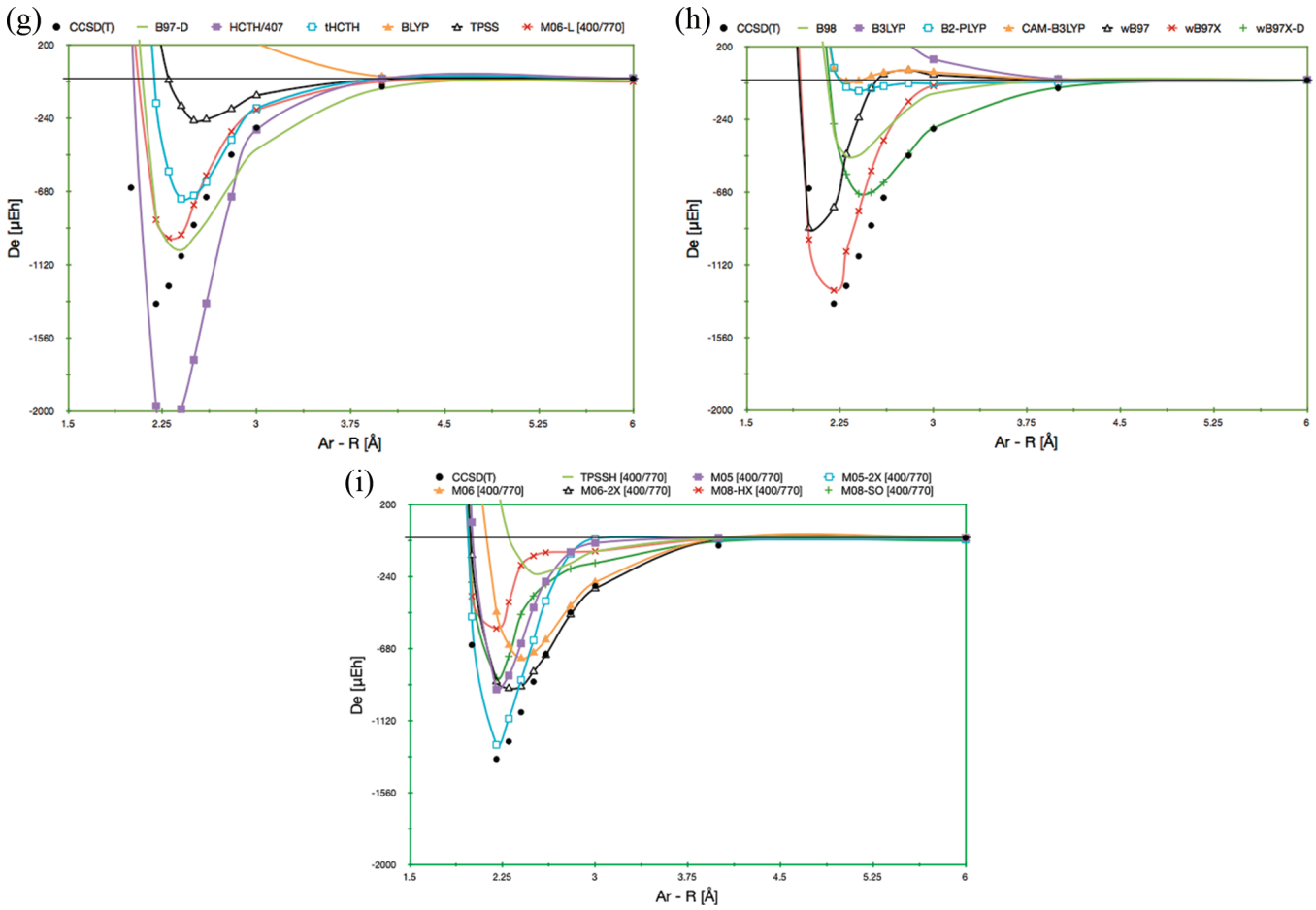

Figure 6. Dissociation energies, D_e (μE_h) of the Rg_3 trimers [a−c, He (blue); d−f, Ne (red); and g−i, Ar (green)] along the radial coordinate R (Å) using the aug-cc-pVTZ basis set together with local GGA [a, d, g], hybrid GGA [b, e, h], and hybrid meta-GGA [c, f, i] DFT functionals, referenced against the CCSD(T)/CBS results in Table 3. Results are presented on the same relative scale; the (96, 1202) Lebedev grid has been used for all but the meta-GGA class of functionals, for which the (400,770) Lebedev grid is used due to the noted oscillatory behavior in these functionals.

BSSE) and requires additional effort, the method generally provides good results for the vast majority of cases where it is used.

Table 6 shows the BSSE as a function of interatomic distance across five common DFT functionals using the aug-cc-pVDZ basis set for the He_3 trimer. The data are expressed as both an absolute value and a percentage of the total binding energy. The absolute value of the BSSE at the binding distance is, in general, larger than 13 μE_h for all of the considered functionals, in the order M06 > B2-PLYP > BMK > BLYP > B3LYP > 13 μE_h. Considering that the dispersion energy near the equilibrium distance, evaluated using the semiempirical dispersion formula of Grimme[33] (namely, the unscaled -D contribution of the B97-D functional), is −140.2 μE_h, the BSSE energy is always larger than 10% of the dispersion energy. With the exception of the B2-PLYP method, the value of the BSSE in the region close to the minimum represents about 5−7% of the total binding energy. The B2-PLYP method, on the other hand, shows a value considerably larger, representing about 35% of the binding energy, with a large basis set dependency. This is most likely due to the presence of the MP2 term. The general behavior of the BSSE with respect to the interatomic distance is fairly unpredictable, ranging significantly across the various functionals, as perhaps seen more clearly in Figure 7. These results show that BSSE plays a substantial role in the determination of the binding energies of the rare gas trimers, particularly with double-ζ quality basis sets, although to a different extent across the functionals.

A reasonable question on the noted effective performance of the BSSE uncorrected combination of DFT and double-ζ quality basis sets arises from this analysis. The proliferation of the use of DFT/double-ζ methods in computational chemistry is primarily due to the relatively cheap computational cost of the combination for a general good performance. However, in many cases, the good performance is amplified by a cancellation of errors in the parametrization of the DFT functional and any associated semiempirical dispersion correction, in combination with the BSSE and the incompleteness of the basis set. In particular, we have previously shown, for small basis sets, that BSSE can be on the same order of magnitude as the dispersion corrections in those functionals that have semiempirical corrections, but the two corrections have different asymptotic behaviors.[41] As such, care should be taken in the selection of the method and basis set, in particular, for computations involving weak interactions. No additional information is revealed in a similar analysis of BSSE effects in the description of the PESs of the other two trimers, Ne_3 and Ar_3. However,

Table 6. BSSE as a Function of Interatomic Distance for Five Common DFT Functionals, Expressed As Absolute Value in μE_h, ABS, and as Percentage of the Total Binding Energy, %

	BLYP		B3LYP		BMK		M06		B2-PLYP	
R	ABS	%	ABS	%	ABS	%	ABS	%	ABS	%
1	60.24	0.31	63.81	0.36	161.38	0.85	295.65	1.80	179.00	1.05
1.2	29.84	0.64	22.38	0.59	30.92	0.52	71.28	2.15	68.56	2.05
1.4	34.63	2.47	29.01	3.15	26.14	0.80	48.94	27.40	54.96	9.08
1.6	24.75	4.30	22.16	6.85	26.98	1.57	54.80	13.84	42.92	30.40
1.65	21.89	4.60	19.16	7.26	25.59	1.88	52.62	11.07	38.14	35.25
1.7	19.26	4.83	15.99	7.27	22.98	2.22	47.98	8.91	32.83	37.52
1.75	17.08	5.00	13.01	6.88	19.46	2.61	41.55	7.38	27.43	36.23
1.8	15.52	5.36	10.53	6.54	15.54	2.92	34.23	7.45	22.40	34.50
1.9	14.34	6.79	7.64	6.43	8.34	3.43	20.31	5.12	14.64	29.74
2	14.92	9.73	7.24	8.37	3.74	4.07	10.49	3.77	10.35	28.80
2.2	15.69	19.45	8.63	19.36	1.37	30.43	2.85	2.21	7.76	45.87
2.4	12.58	28.70	7.74	33.34	1.49	39.72	1.37	2.34	6.18	84.21
2.6	8.08	32.54	5.28	41.92	1.17	38.03	0.68	2.81	4.09	130.13
2.8	4.50	30.52	3.09	42.36	0.75	41.23	0.33	2.95	2.37	165.88
3	2.24	23.91	1.61	35.05	0.44	53.45	0.19	3.48	1.25	159.86

all tables and graphics associated with this analysis are available as Supporting Information, for those interested in the details.

Conclusions

A systematic investigation into potential energy surfaces characteristics of a series of rare gas trimers across a wide range of methodologies has been presented. Because of the much smaller amount of literature compared to that for rare gas dimer counterparts, it is of interest to investigate this series for a better understanding of *n*-body interaction energies, but also for the evaluation of model chemistries.

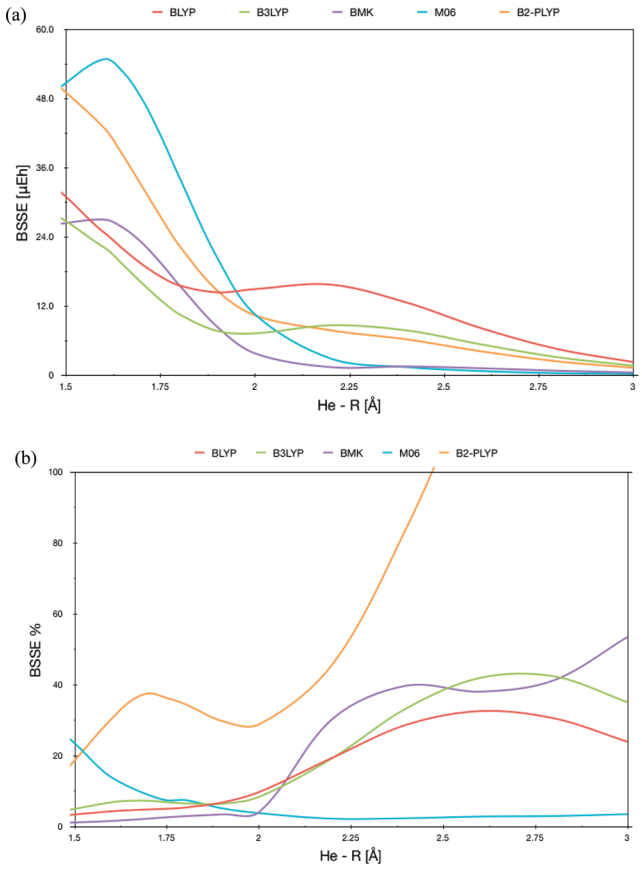

Figure 7. BSSE as a functional of interatomic distance, expressed as (a) absolute value and (b) percentage of the total binding energy.

In the equilateral D_{3h} case, the trimer series presents a simple one-dimensional potential energy surface, from which the methodology can be compared. These systems represent a challenging test for new methodologies, as all three trimers are van der Waals, or dispersion-bound, systems, with varying degrees of atomic polarizability.

For this study, we have implemented a large set of Kohn−Sham DFT density functionals into the GAMESS software package to fully test performance across a wide range of functional class types, including several of the new dispersion enabled functional strategies. In the process, we also facilitate future implementations and parameter testing of a variety of density functional types. Reference data for the He_3 trimer are investigated in detail using CCSD(T) dissociation energies, D_e (μE_h), of the trimer along the radial coordinate R (Å) for the aug-cc-pVnZ ($n = 2-5$) series of basis sets and CBS extrapolation. Several well-established extrapolation procedures are compared. Optimal results are achieved with the exponential [TQ5;Feller]-CBS and the simple two-point [Q5;Schwartz]-CBS extrapolation procedures. The [TQ5;Feller]-CBS was subsequently used to establish reference calculations for all three rare gas trimer systems.

Benchmarked against the reference data, investigation is then made across a set of 34 DFT functionals of varying classes, evaluated on the same PES points, using double- and triple-ζ quality basis sets, for all three rare gas trimers. Results with and without correction for basis set superposition error are discussed. Because of spurious oscillation in the potential energy surfaces obtained with meta-GGA functionals, a detailed investigation of the DFT integration grid was also carried out. The tightest grid, (400, 700), was used for all meta-GGA reported results reported here. In general, we propose a sequence of increasing accuracy in terms of (radial, angular) points for Lebedev-type integration grids, as (96,302), (125,590), (250,770), and potentially (400,770), however such a large radial component can easily be overkill, resulting in no additional convergence, but considerable CPU time.

Criteria for the evaluation of calculated potentials for any method on systems of this type should encompass good prediction of the equilibrium distance, dissociation energy,

and long-range behavior. However, what we see from the reported results across DFT classes is that predictions strongly vary depending on the rare gas system, such that no unique best functional can be recommended across the whole series. Local functionals provide a generally poor behavior across all criteria, while hybrid GGAs are somewhat better overall. Meta-GGA functionals are largely unsatisfactory but still represent the best functionals in specific cases, for one or more of the criteria. Oscillations in the behavior of the PES are found for many meta-GGA functionals, despite the use of an ultrafine Lebedev integration grid. We therefore suggest that these functionals be used with caution. A correct long-range behavior should fit to a $c_6/r^6 + c_8/r^8$ like behavior, as is expected from the semiempirical, -D, corrected versions of the functionals, which do quite well for the Rg_2 dimer systems. However, only a few of the potentials calculated with the semiempirically corrected functionals have better long-range behavior, probably the best example being ωB97X-D. The newly implemented range-separated hybrids and semiempirical corrected functionals project the most reasonable global results, relatively speaking. The same does not hold for the B2-PLYP double hybrid functional, which performs quite poorly for all considered cases. The trends in BSSE were considered in more detail, posing a reasonable question on the effective performance of the BSSE uncorrected combination of DFT with double-ζ quality basis sets.

Acknowledgment. We gratefully acknowledge the University of Zürich and the Swiss National Science Foundation for support of this research. We thank M. W. Schmidt for his helpful discussions.

Supporting Information Available: Summary of newly implemented DFT functionals in GAMESS, categorized by DFT class type; CCSD(T) dissociation energies, D_e (μE_h), of the He_3 molecule along the radial coordinate R (Å) for various basis sets and CBS extrapolation formulas; weights used in the wMAD in accord with the shape of the accurate CCSD(T)/CBS PES; MAD, wMAD, and deviation from reference near the equilibrium distance for 34 different density functionals; BSSE as a function of interatomic distance for five common DFT functionals. This material is available free of charge via the Internet at http://pubs.acs.org.

References

(1) Efimov, V. *Phys. Lett.* **1970**, *33B*, 563.

(2) Efimov, V. *Nucl. Phys. A.* **1973**, *210*, 157.

(3) Efimov, V. *Comments Nucl. Part. Phys.* **1990**, *19*, 271.

(4) Suno, H.; Esry, B. D. *Phys. Rev. A* **2008**, *78*, 062701.

(5) Richard, J. M. *Few-Body Syst.* **2006**, *38*, 79–84.

(6) Zhukov, M. V.; Danilin, B. V.; Fedorov, D. V.; Bang, J. M.; Thompson, I. S.; Vaagen, J. S. *Phys. Rep.* **1993**, *231*, 151.

(7) Cybulski, S. M.; Toczlowski, R. R. *J. Chem. Phys.* **1999**, *111*, 10520.

(8) Bressanini, D.; Morosi, G. *Phys. Rev. A* **2003**, *90*, 133401.

(9) Bressanini, D.; Morosi, G. *Few-Body Syst.* **2004**, *34*, 1–3.

(10) Cencek, W.; Jeziorska, M.; Akin-Ojo, O.; Szalewicz, K. *J. Phys. Chem. A.* **2007**, *111*, 11311.

(11) Cencek, W.; Patkowski, K.; Szalewicz, K. *J. Chem. Phys.* **2009**, *131*, 064105.

(12) Giese, T.; York, D. M. *Int. J. Quantum Chem.* **2004**, *98*, 388–408.

(13) Giese, T.; York, D. M. *J. Chem. Phys.* **2004**, *120*, 590.

(14) Ichihara, A.; Itoh, A. B. *Chem. Soc. Jpn.* **1990**, *63*, 958–960.

(15) Kim, Y. S. *Phys. Rev. A* **1975**, *11*, 796–803.

(16) Blume, D.; Greene, C. H.; Esry, B. D. *J. Chem. Phys.* **2000**, *113*, 2145.

(17) Chakravarty, C.; Hinde, R. J.; Leitner, D. M.; Wales, D. J. *Phys. Rev. E* **1997**, *56*, 563.

(18) González-Lezana, T.; Rubayo-Soneira, J.; Miret-Artés, S.; Gianturco, F. A.; Delgado-Barrio, G.; Villarreal, P. *J. Chem. Phys.* **1999**, *110*, 9000.

(19) Bruch, L. W.; Novaro, O.; Flores, A. *J. Chem. Phys.* **1977**, *67*, 2371.

(20) Lim, T. K.; Duffy, K.; Nakaichi, S.; Akaishi, Y.; Tanaka, H. *J. Chem. Phys.* **1979**, *70*, 4782.

(21) Sandhas, W.; Kolganova, E. A.; Ho, Y. K.; Motovilov, A. K. *Few-Body Syst.* **2004**, *34*, 137.

(22) Zhao, Y.; Schultz, N. E.; Truhlar, D. G. *J. Chem. Phys.* **2005**, *123*, 161103/1–161103/4.

(23) Zhao, Y.; Truhlar, D. G. *Acc. Chem. Res.* **2008**, *41*, 157–167.

(24) Zhao, Y.; Truhlar, D. G. *Theor. Chem. Acc.* **2008**, *120*, 215–241.

(25) Zhao, Y.; Truhlar, D. G. *J. Chem. Theory Comput.* **2008**, *4*, 1849.

(26) Boese, A. D.; Handy, N. C. *J. Chem. Phys.* **2002**, *116*, 9559–9569.

(27) Boese, A. D.; Martin, J. M. L. *J. Chem. Phys.* **2004**, *121*, 3405.

(28) Leininger, T.; Stoll, H.; Werner, H. J.; Savin, A. *Chem. Phys. Lett.* **1997**, *275*, 151–160.

(29) Yanai, T. *Chem. Phys. Lett.* **2004**, *393*, 51–57.

(30) Hetzer, G.; Pulay, P.; Werner, H.-J. *Chem. Phys. Lett.* **1998**, *290*, 143.

(31) Heyd, J.; Scuseria, G. E. *J. Chem. Phys.* **2004**, *120*, 7274.

(32) Chai, J. D.; Head-Gordon, M. *J. Chem. Phys.* **2008**, *108*, 084106.

(33) Grimme, S. *J. Comput. Chem.* **2006**, *27*, 1787–1799.

(34) Grimme, S. *J. Chem. Phys.* **2006**, *124*, 034108−034115.

(35) Schwabe, T.; Grimme, S. *Phys. Chem. Chem. Phys.* **2006**, *8*, 4398–4401.

(36) Zhao, Y.; Lynch, B. J.; Truhlar, D. G. *J. Phys. Chem. A.* **2004**, *108*, 4786.

(37) Tarnopolsky, A.; Karton, A.; Sertchook, R.; Vuzman, D.; Martin, J. M. L. *Phys. Chem. A* **2008**, *112*, 3–8.

(38) Dion, M.; Rydberg, H.; Schröder, E.; Langreth, D. C.; Lundqvist, B. I. *Phys. Rev. Lett.* **2004**, *92*, 246401.

(39) Bode, B. M.; Gordon, M. S. *Mol. Graphics Modell.* **1999**, *16*, 133–138.

(40) Tarini, M.; Cignoni, P.; Montani, C. *IEEE Trans. Visual. Comput. Graphics* **2006**, *12*, 1237–1244.

(41) Peverati, R.; Baldridge, K. K. *J. Chem. Theory Comput.* **2008**, *4*, 2030–2048.

(42) Becke, A. D. *J. Chem. Phys.* **1997**, *107*, 8554–8560.

(43) Hamprecht, F. A.; Cohen, A. J.; Tozer, D. J.; Handy, N. C. *J. Chem. Phys.* **1998**, *109*, 6264–6271.

(44) Keal, T. W.; Tozer, D. J. *J. Chem. Phys.* **2005**, *123*, 121103.

(45) Wilson, P. J.; Bradley, T. J.; Tozer, D. J. *J. Chem. Phys.* **2001**, *115*, 9233–9242.

(46) Strange, R.; Manby, F. R.; Knowles, P. J. *Comput. Phys. Commun.* **2001**, *136*, 310–318.

(47) Miehlich, B.; Stoll, H.; Savin, A. *Mol. Phys.* **1997**, *91*, 527.

(48) Becke, A. D. *J. Chem. Phys.* **1998**, *108*, 9624–9631.

(49) Boese, A. D.; Doltsinis, N. L.; Handy, N. C.; Sprik, M. *J. Chem. Phys.* **2000**, *112*, 1670–1678.

(50) Boese, A. D.; Handy, N. C. *J. Chem. Phys.* **2001**, *114*, 5497–5503.

(51) Becke, A. D. *Phys. Rev. A* **1988**, *38*, 3098.

(52) Lee, C.; Yang, W.; Parr, R. G. *Phys. Rev. B* **1988**, *37*, 785–789.

(53) Miehlich, B.; Savin, A.; Stoll, H.; Preuss, H. *Chem. Phys. Lett.* **1989**, *157*, 200–206.

(54) Stephens, P. J.; Devlin, F. J.; Chablowski, C. F.; Frisch, M. J. *J. Phys. Chem.* **1994**, *98*, 11623–11627.

(55) Hertwig, R. H.; Koch, W. *Chem. Phys. Lett.* **1997**, *268*, 345–351.

(56) van Voorhis, T.; Scuseria, G. E. *J. Chem. Phys.* **1998**, *109*, 400–410.

(57) Perdew, J. P.; Kurth, S.; Zupan, A.; Blaha, P. *Phys. Rev. Lett.* **1999**, *82*, 2544–2547.

(58) Tao, J. M.; Perdew, J. P.; Staroverov, V. N.; Scuseria, G. E. *Phys. Rev. Lett.* **2003**, *91*, 146401–146404.

(59) Perdew, J. P.; Tao, J. M.; Staroverov, V. N.; Scuseria, G. E. *J. Chem. Phys.* **2004**, *120*, 6898–6911.

(60) Staroverov, V. N.; Scuseria, G. E.; Tao, J.; Perdew, J. P. *J. Chem. Phys.* **2003**, *119*, 12129–12137.

(61) Staroverov, V. N.; Scuseria, G. E.; Tao, J.; Perdew, J. P. *J. Chem. Phys.* **2004**, *121*, 11507.

(62) Perdew, J. P.; Ruzsinszky, A.; Tao, J.; Csonka, G. I.; Scuseria, G. E. *Phys. Rev. A* **2007**, *76*, 042506−042511.

(63) Zhao, Y.; Truhlar, D. G. *J. Chem. Theory Comput.* **2006**, *2*, 1009–1018.

(64) Zhao, L.; Truhlar, D. G. *J. Chem. Phys.* **2006**, *125*, 194101–194119.

(65) Zhao, Y.; Truhlar, D. G. *J. Phys. Chem. A.* **2006**, *110*, 13126–13130.

(66) Lebedev, V. I.; Laikov, D. N. *Dokl. Math.* **1999**, 477–478.

(67) Su, P.; Li, H. *J. Chem. Phys.* **2009**, *131*, 014102.

(68) Møller, C.; Plesset, M. S. *Phys. Rev.* **1934**, *46*, 618–622.

(69) Piecuch, P.; Kucharski, S. A.; Kowalski, K.; Musial, M. *Comput. Phys. Commun.* **2002**, *149*, 71–96.

(70) Bentz, J. L.; Olson, R. M.; Gordon, M. S.; Schmidt, M. W.; Kendall, R. A. *Comput. Phys. Commun.* **2007**, *176*, 589–600.

(71) Olson, R. M.; Bentz, J. L.; Kendall, R. A.; Schmidt, M. W.; Gordon, M. S. *J. Comput. Theor. Chem.* **2007**, *3*, 1312–1328.

(72) Dunning, T. H. *J. Chem. Phys.* **1989**, *90*, 1007–1023.

(73) de Lara-Castellis, M. P.; Krems, R. V.; Buchachenko, A. A.; Delgado-Barrio, G.; Villarreal, P. *J. Chem. Phys.* **2001**, *115*, 10438.

(74) Feller, D. F.; Sordo, J. A. *J. Chem. Phys.* **2000**, *112*, 5604.

(75) Halkier, A.; Helgaker, T.; Jørgensen, P.; Klopper, W.; Koch, H.; Olsena, J.; Wilson, A. K. *Chem. Phys. Lett.* **1998**, *286*, 243.

(76) Martin, J. M. L. *Chem. Phys. Lett.* **1996**, *262*, 97–104.

(77) Martin, J. M. L. *Chem. Phys. Lett.* **1996**, *259*, 669–678.

(78) Martin, J. M. L. *Chem. Phys. Lett.* **1998**, *292*, 411.

(79) Martin, J. M. L.; Taylor, P. R. *J. Chem. Phys.* **1997**, *106*, 8620–8623.

(80) Nyden, M. R.; Petersson, G. A. *J. Chem. Phys.* **1981**, *75*, 1843.

(81) Peterson, K. A.; Dunning, T. H., Jr. *J. Phys. Chem. A* **1997**, *101*, 6280–6292.

(82) Peterson, K. A.; Woon, D. E.; Dunning, T. H., Jr. *J. Chem. Phys.* **1994**, *100*, 7410.

(83) Petersson, G. A.; Bennett, A.; Tensfeldt, T. G.; Al-Laham, M. A.; Shirley, W. A.; Mantzaris, J. *J. Chem. Phys.* **1988**, *89*, 2193.

(84) Petersson, G. A.; Frisch, M. J. *J. Phys. Chem. A* **2000**, *104*, 2183.

(85) Petersson, G. A.; Yee, A. K.; Bennett, A. *J. Chem. Phys.* **1985**, *83*, 5105.

(86) Schwartz, C. *Phys. Rev.* **1962**, *126*, 1015.

(87) Schwartz, C. *Computaitonal Physics*; Academic: New York, 1963; Vol. 2.

(88) Truhlar, D. G. *Chem. Phys. Lett.* **1998**, *294*, 45–48.

(89) Wilson, A. K.; Dunning, T. H., Jr. *J. Chem. Phys.* **1997**, *106*, 8718.

(90) Woon, D. E.; Dunning, T. H., Jr. *J. Chem. Phys.* **1994**, *100*, 2975.

(91) Martin, J. M. L. *Chem. Phys. Lett.* **1996**, *259*, 679–682.

(92) van Mourik, T.; van Lenthe, J. H. *J. Chem. Phys.* **1995**, *102*, 7479.

(93) Komasa, J.; Rychlewski, J. *Mol. Phys.* **1997**, *91*, 909.

(94) Burda, J. V.; Zahradnik, R.; Hobza, P.; Urban, M. *Mol. Phys.* **1996**, *89*, 425.

(95) Korona, T.; Williams, H. L.; Bukowski, R.; Jeziorski, B.; Szalewicz, K. *J. Chem. Phys.* **1997**, *106*, 5109.

(96) Specchio, R.; Famulari, A.; Raimondi, M. *THEOCHEM* **2001**, *549*, 77.

(97) Gdanitz, R. J. *Chem. Phys. Lett.* **2001**, *348*, 67.

(98) Cybulski, S. M.; Toczłowski, R. R. *J. Chem. Phys.* **1999**, *111*, 10520.

(99) Aziz, R. A.; Slaman, M. *Chem. Phys.* **1989**, *130*, 187–194.

(100) Aziz, R. A. *J. Chem. Phys.* **1993**, *99*, 4518.

(101) Jansen, H. B.; Ross, P. *Chem. Phys. Lett.* **1969**, *3*, 140.

(102) Johnson, E. R.; Becke, A. D.; Sherrill, C. D.; DiLabio, G. A. *J. Chem. Phys.* **2009**, 131.

(103) Johnson, E. R.; Wolkow, R. A.; DiLabio, G. A. *Chem. Phys. Lett.* **2004**, *394*, 334.

(104) Wheeler, S. E.; Houk, K. N. *J. Chem. Theory Comput.* **2010**, DOI: 10.1021/ct900639.

(105) Dunlap, B. I. *J. Phys. Chem.* **1986**, *90*, 5524.

(106) Werpetinski, K. S.; Cook, M. *Phys. Rev. A* **1997**, *52*, R3397.

(107) Wheeler, S. E.; Houk, K. N. *J. Chem. Theory Comput.* **2009**, *5*, 2301.

(108) Murray, C. W.; Handy, N. C.; Laming, G. L. *Mol. Phys.* **1993**, *78*, 997–1014.

(109) Treutler, O. T.; Ahlrichs, R. *J. Chem. Phys.* **1995**, *102*, 346.

(110) Wang, X.-G.; Carrington Jr, T. *J. Theor. Comput. Chem.* **2003**, *2*, 599–608.

(111) Lebedev, V. I. *Zh. Vychisl. Mat. Mat. Fiz.* **1975**, *15*, 48.

(112) Lebedev, V. I. *Zh. Vychisl. Mat. Mat. Fiz.* **1975**, *16*, 293.

(113) Kestner, N. R.; Combariza, J. E. In *Reviews in Computational Chemistry*; Boyd, D. B., Lipkowitz, K. B., Eds.; Wiley-VCH: New York, 1999; Vol. 13, pp 99−132.

(114) Grimme, S. *J. Comput. Chem.* **2004**, *25*, 1463–1473.

(115) Paizs, B.; Suhai, S. *J. Comput. Chem.* **1998**, *19*, 575–584.

CT100061F